

# JAAS

Accepted Manuscript



This is an *Accepted Manuscript*, which has been through the Royal Society of Chemistry peer review process and has been accepted for publication.

*Accepted Manuscripts* are published online shortly after acceptance, before technical editing, formatting and proof reading. Using this free service, authors can make their results available to the community, in citable form, before we publish the edited article. We will replace this *Accepted Manuscript* with the edited and formatted *Advance Article* as soon as it is available.

You can find more information about *Accepted Manuscripts* in the [Information for Authors](#).

Please note that technical editing may introduce minor changes to the text and/or graphics, which may alter content. The journal's standard [Terms & Conditions](#) and the [Ethical guidelines](#) still apply. In no event shall the Royal Society of Chemistry be held responsible for any errors or omissions in this *Accepted Manuscript* or any consequences arising from the use of any information it contains.

1  
2  
3 **Accumulation and biotransformation of chitosan-modified selenium nanoparticles in**  
4 **exposed Radish (*Raphanus sativus*).**  
5  
6  
7

8 Maria Palomo-Siguero, Maria Isabel López-Heras, Carmen Cámara and Yolanda Madrid\*  
9 Departamento de Química Analítica. Facultad de Ciencias Químicas. Universidad  
10 Complutense de Madrid. 28040 Madrid. Spain.  
11  
12  
13

14  
15  
16 **Abstract.**  
17

18 In this investigation, we evaluate the biotransformation of chitosan- modified SeNPs (CS-  
19 SeNPs) in radish plants (*Raphanus sativus*) by using an analytical methodology which  
20 combines high performance liquid chromatography (HPLC) and asymmetrical flow field flow  
21 fractionation (AF<sup>4</sup>) on line coupled to inductively coupled plasma mass spectrometry (ICP-  
22 MS), as well as transmission electron microscopy (TEM). CS-SeNPs were synthesized using  
23 a solution-phase approach based on the reduction of selenite with ascorbic acid in the  
24 presence of chitosan as stabilizer agent. The average diameter of the resulting spherical CS-  
25 SeNPs was 26±3nm. Extracts of radish plants exposed to CS-SeNPs were analyzed by  
26 HPLC-ICPMS and the results shown that a percentage higher than 95 % of the selenium  
27 accumulated was biotransformed in MeSeCys and SeMet. We assume that CS-SeNPs are  
28 first adsorbed on the root system and then transformed to organic selenium compounds  
29 following a similar metabolic pathway to selenite. Characterization of CS-SeNPs diameter  
30 size in radish root system was performed by using both AF<sup>4</sup>-UV-ICPMS and TEM. The size  
31 distributions, determined by TEM, were in good agreement with that obtained from AF<sup>4</sup>-  
32 ICPMS. The results are of importance since the number of applications of AF<sup>4</sup>-ICPMS to  
33 diameter size estimation of nanoparticles in living systems is still scarce. To the best of our  
34 knowledge, this is the first report confirming the biotransformation of SeNPs in plants.  
35  
36  
37  
38  
39  
40  
41  
42  
43  
44  
45  
46

47 \*To whom correspondence should be addressed.

48 Email: ymadrid@quim.ucm.es  
49  
50  
51  
52  
53  
54  
55  
56  
57  
58  
59  
60

## 1. Introduction

Selenium as a component of seleno amino acids and selenoproteins is essential in important physiological functions: stimulation of the immune system, redox homeostasis and thyroid hormone metabolism. Selenium deficiency has been also associated to a range of diseases, such as muscle and cardiovascular disorders, cancer, and neurological and endocrine function disorders<sup>1,2</sup>. Moreover, several studies have suggested that some organic forms of selenium could show anticarcinogenic properties against certain types of cancer<sup>3</sup>. Even though the mechanisms involved in cancer inhibition are still unclear, being tentatively attributed to biological functions of seleno amino acids, such as Se-methylselenocysteine (MeSeCys). However, a higher Se intake than recommended can result in adverse health effects. Therefore, Se has either nutritional function or toxicity depending on its concentration and species. Therefore, how to provide efficient and safe application of dietary selenium supplementation has become a challenge topic in recent years.

Nanotechnology has been touted as the next revolution in many industries, including food processing and packaging. The applications of nano-based technology in food industry may include nano scale vehicles for delivering nutrients and sensitive bioactives, nanoscale films for food packaging and contact materials, nanoscale systems for controlled releasing of fertilizer and pesticides, safety and biosecurity (e.g. nanosensors), and nanotoxicity. Based on these advances, nanotechnology could be also applied for developing selenium nanoparticles as a vehicle for delivering selenium in living systems.

Selenium nanoparticles (SeNPs), which can be considered a novel Se compound, has shown to have excellent antioxidants properties and low toxicity when comparing with other Se-species such as SeMet and MeSeCys. The acute toxicity (LD<sub>50</sub>) of Nano-Se in mice (92.1 mg Se/kg, 95% confidence limits 71.1–131.1) is significantly lower than that of selenite (15 mg/kg) and SeMet (25.6 mg Se/kg). Selenite and selenomethionine were more active than Nano-Se (36nm averaged diameter size) in increasing serum alanine aminotransferase and aspartate aminotranferase activities, two biomarkers of liver toxicity caused by selenium, as well as in inducing other signs of liver toxicity.<sup>4</sup> Moreover, it has been reported that SeNPs induce cell cycle arrest in HepG2 cancer cells growth. Data suggest that cell cycle of HepG2 cells is arrested at the S phase by alteration of the eIF3 protein complex expression as result

1  
2  
3 of Ch-SeNPs exposure, which may hampers translation of mRNAs responsible for encoding  
4 proteins important for cell proliferation and oncogenesis<sup>5</sup>  
5  
6  
7

8 Most of the studies concerning selenium nanoparticles are mainly focused on the interaction  
9 of SeNPs with biological systems, being their potential in food and agriculture less explored.  
10 Romero *et al*<sup>6</sup> administrate SeNPs enriched- feed to evaluate its further possible use to  
11 improve selenium absorption in ruminants. Sodium selenite was encapsulated by  
12 nanoprecipitation and emulsion–evaporation methods, within polymeric nanoparticles of  
13 Eudragit RL. The high release of ionic selenium from nanoparticles in acid media (pH< 4)  
14 suggests a better bioavailability of the element in the small intestine. Uptake, accumulation  
15 and biological effects of red nano-size elemental selenium in tobacco callus cultures and  
16 rooted tobacco plants were evaluated by Domokos-Szabolcsy *et al*<sup>7</sup>. SeNPs were produced  
17 by *Lactobacillus acidophilus* grown in Selenite enriched medium. The biological effects  
18 observed in plant tissues exposed to nanoSe were different than those exposed to selenate.  
19 NanoSe (265–530 mM concentration range) stimulated the organogenesis and the growth of  
20 root system significantly (40 %).  
21  
22  
23  
24  
25  
26  
27  
28  
29  
30

31 In the present study, biotransformation of chitosan-modified SeNPs in hydroponic radish  
32 plants (*Raphanus sativus*) was investigated by using several analytical methods. Selenium  
33 nanoparticles were synthesized using a solution-phase approach based on the reduction of  
34 selenite with ascorbic acid in presence of chitosan (CS) as modifier or stabilizer agent. An  
35 analytical methodology which combines the use of HPLC and AF<sup>4</sup> coupled to ICPMS as well  
36 as transmission electron microscopy (TEM) was employed to characterize the CS-SeNPs and  
37 to establish their accumulation and biotransformation in radish plants. Results obtained were  
38 compared with those provide by radish plants hydroponically grown in presence of selenite<sup>8</sup>.  
39 The study also evaluates the capability of AF<sup>4</sup>-ICPMS to characterize diameter size of SeNPs  
40 in living system. This research will facilitate the understanding of the transformation of  
41 nanomaterials and forecasting their fate and toxicity in the environment and biological  
42 systems. In summary, it will allow us to evaluate selenium nanoparticles as a way of  
43 delivering selenium in food and agriculture areas.  
44  
45  
46  
47  
48  
49  
50  
51  
52  
53  
54  
55  
56  
57  
58  
59  
60

## 2. Experimental

### 2.1 Chemicals and instrumentation

All chemicals and reagents used were of analytical grade and solutions were prepared with de-ionized water (18 M  $\Omega$  cm) obtained from a Milli-Q water purification system unit (Millipore, USA). Stock standard solutions of SeMet, MeSeCys and SeCys<sub>2</sub> (Sigma-Aldrich, Germany), were prepared by dissolving them in 3% hydrochloric acid (37%, Merck, Germany). Inorganic selenium solutions were prepared by dissolving sodium selenite (Na<sub>2</sub>SeO<sub>3</sub>) and selenate (Na<sub>2</sub>SeO<sub>4</sub>), purchased from Merck, in Milli-Q water. Stock solutions of 1000 mgL<sup>-1</sup> were stored at 4 °C, whereas working standard solutions were prepared daily by dilution.

Chitosan polysaccharide and ascorbic acid purchased from Sigma Aldrich and acetic acid from Fluka were used for Chitosan modified-SeNPs synthesis.

Enzymatic hydrolysis was carried out using a non-specific enzyme, Protease XIV from *Streptomyces griseus*. Tris-HCl buffer solution used for species extraction was prepared by Trizma base (Fluka) dissolution in water at pH 7.5 adjusted with HCl.

Selenium species separation by anionic-exchange chromatography was achieved by using 10 mM citric acid (Sigma) in 2% MeOH (99.9%, Scharlau) adjusted to pH 5 with ammonium hydroxide (Fluka) as mobile phase. The mobile phase for Zorbax C8 reversed-phase chromatography was 0.1% trifluoroacetic acid, TFA (Sigma-Aldrich), in 2% MeOH.

A 1000W MSP microwave oven (CEM, Matthews, NC) equipped with temperature and pressure feedback controllers and 12 high pressure vessels of 100 mL inner volume, operating at a maximum power of 1600W was used for microwave acid digestion.

A Sonoplus ultrasonic homogenizer (Bandelin, Berlin, Germany) equipped with a 3-mm diameter titanium microtip fitted with a high-frequency generator of 2200W at a frequency of 20 kHz, and an ultrasonic bath (JP Selecta, Barcelona, Spain), were used to extract the seleno-compounds from the plant tissues

An Agilent 7700-collision/reaction cell ICP-MS (using H<sub>2</sub> collision gas) (Agilent Technologies, Santa Clara, CA) was employed for elemental specific detection. HPLC-ICP-MS measurements were carried out using a PU-2089 LC pump (JASCO, Tokyo, Japan) fitted

1  
2  
3 with a six-port injection valve (model 7725i, Rheodyne, Rohner Park, CA,) with a 100- $\mu$ L  
4 injection loop for the chromatographic separations.  
5  
6

7  
8 Two different chromatographic columns were used: anionic exchange PRP-X100 (250 x 4.1  
9 mm, 10  $\mu$ m) (Hamilton, Switzerland) and a reversed-phase ion pairing C8 Zorbax R<sub>x</sub>-C<sub>8</sub> (250  
10 x 3.0 mm, 5  $\mu$ m) (Agilent, USA). The outlet of the column was connected directly into the  
11 conical nebulizer of the ICP-MS with PEEK tubing. The operating parameters are compiled  
12 in Table 1.  
13  
14  
15  
16

17  
18 An asymmetrical flow field flow fractionation (AF<sup>4</sup>) AF2000 system (Postnova Analytik,  
19 Landsberg, Germany), equipped with a regenerated cellulose membrane of 10 kDa molecular  
20 weight cut-off and a spacer of 500 nm, was used in this study. A loop of 200  $\mu$ l was  
21 employed to inject the samples into the AF<sup>4</sup> via a Rheodyne valve. The AF<sup>4</sup> channel was  
22 connected on-line to a UV detector (Model 1260 Infinity; Agilent Technologies) and to an  
23 ICPMS. The optimized AF<sup>4</sup> settings and flows used for the separations, and the UV and  
24 ICPMS detection operating conditions are detailed in Table 1. The AF<sup>4</sup> system was also  
25 calibrated for molecular diameter size determination by using polystyrene latex (PSL) beads  
26 reference standards of three known sizes (22, 54 and 100 nm).  
27  
28  
29  
30  
31  
32

33 Characterization of the synthesized CSSeNPs was performed by using a high resolution  
34 transmission electron microscope (JEOL JEM 2100, USA) equipped with a X-Ray energy  
35 dispersive spectroscopy (XEDS) microanalysis composition system (Oxford Inca). Samples  
36 for TEM analysis were prepared by evaporating a drop of chitosan-modified SeNPs or a drop  
37 of radish extracts onto a 300 mesh lacey carbon copper grid.  
38  
39  
40  
41  
42  
43  
44

## 45 **2.2. Synthesis of chitosan-modified selenium nanoparticles**

46  
47

48 Chitosan modified-SeNPs (CS-SeNPs) were prepared according to the procedure described  
49 by Bay *et al*<sup>9</sup>. Firstly, aqueous chitosan solutions within the concentration range from 0.01  
50 to 0.5% (w/v) were prepared in 3% (w/v) acetic acid solution. Then, ascorbic acid was added  
51 dropwise into chitosan-acetic acid mixture and magnetically stirred for about 30 minutes at  
52 room temperature. After that, sodium selenite was slowly added to the chitosan-acetic-  
53 ascorbic acid mixture and stirred for 30 minutes. Finally the dispersion was diluted to 100  
54  
55  
56  
57  
58  
59  
60

mL with distilled water obtaining a final concentration of 200 mg L<sup>-1</sup> of chitosan-modified selenium nanoparticles. Synthesized CS-SeNPs were stored at 4°C up to two months.

The efficiency of nanoparticles formation was calculated by ICPMS measurements, after a mass balance of the amount of selenium added and the amount of free selenium obtained after filtering the suspension with a 10kDa molecular weight cut off filter by applying centrifugation at 400g for 30 min at room temperature.

### 2.3 Plant Growth and Samples.

Experiments were conducted in a greenhouse under controlled conditions of temperature and light. Seeds of radish (*R. sativus*) were germinated in darkness at 25°C on filter paper moistened with water in Petri dishes. After 5 days- germination, seedlings were transferred to 300 mL plastic vessels with modified Hoagland's nutrient solution (0.1 strength and pH 5.6) containing: 0.2M KH<sub>2</sub>PO<sub>4</sub>; 1M KNO<sub>3</sub>; 0.8M Ca(NO<sub>3</sub>)<sub>2</sub>·4H<sub>2</sub>O; 0.4M MnSO<sub>4</sub>·7H<sub>2</sub>O, 0.02M Fe-EDDHA; 0.02M H<sub>3</sub>BO<sub>3</sub>; 0.004 MnSO<sub>4</sub>·5H<sub>2</sub>O; 0.0004M ZnSO<sub>4</sub>·7H<sub>2</sub>O; 0.0004 CuSO<sub>4</sub>·5H<sub>2</sub>O; 0.0002M Na<sub>2</sub>MoO<sub>4</sub>·2H<sub>2</sub>O, using perlite as substrate during 2 weeks. Afterwards, Selenium as selenite and SeNPs (1 mg L<sup>-1</sup> each) were added to the vessels, and solutions were renewed every 3 days for 40 days, until the cycle of the plants was completed. A control group of plants without adding selenium was grown in parallel. Then, plants were harvested and washed with de-ionized water. Radish samples were chopped and stored at 4°C before analysis.

### 2.4 Selenium Analysis

**2.4.1. Total Selenium Determination.** About 250 mg of fresh radish sample were microwave digested with 2.5 mL of concentrated HNO<sub>3</sub> and 1 mL of 30% hydrogen peroxide to determine the total selenium content. The resulting solution was diluted to 25 mL with deionized water and selenium concentration was determined by ICP-MS following operating conditions given in Table 1. Results are expressed as the mean value (standard deviation for *n* =3).

**2.4.2. Selenium species determination.** Selenium species extraction from 250 mg of fresh radish samples was performed by using enzymatic probe sonication<sup>8</sup> after adding 3 mL of de-ionized water and 10 mg of Protease XIV. The extracts were centrifuged at 7500g for 30 min using a 10 kDa cutoff filter. The extracts were analyzed by HPLC-ICPMS using two



1  
2  
3 different chromatographic separation mechanisms: anion exchange chromatography and  
4 reversed- phase chromatography and by following the experimental conditions given in Table  
5 1. Recovery of the selenium compounds on the column was evaluated using column  
6 switching on the HPLC set up in a flow injection mode. To determine the column recovery of  
7 the injected selenium compound standards, the flow injection peak areas obtained were  
8 compared with the peak areas of the chromatogram. Selenium species concentration was  
9 determined by monitoring  $^{76}\text{Se}$ ,  $^{77}\text{Se}$ ,  $^{78}\text{Se}$ , and  $^{80}\text{Se}$  isotopes using the standard addition  
10 method.

11  
12 Method accuracy was evaluated by using an enriched wheat flour reference material (ERM  
13 BC210a), certified for selenium ( $17.23 \pm 0.91 \mu\text{g g}^{-1}$ ) and selenomethionine content ( $27.4 \pm 2.6$   
14  $\mu\text{g g}^{-1}$ ), from LGC (United Kingdom)  
15

16  
17  
18 **2.4.3. AF<sup>4</sup>-UV-ICPMS and TEM detection of chitosan modified- selenium**  
19 **nanoparticles in radish root system.** CS-SeNPs were extracted from the radish root system  
20 by using the medium employed in the CS-SeNPs synthesis (0.1% Chitosan, 0.034M Ascorbic  
21 acid, 0.24M Acetic acid) as extracting solution. To about 200 mg of fresh radish samples,  
22 1mL of extracting solution were added and followed by 30 min of sonication in an ultrasonic  
23 bath. The resulting extracts were centrifuged at 10000rpm for 10 min and analyzed by TEM  
24 and X-Ray Energy Dispersive Spectroscopy (XEDS) for the microanalysis composition.  
25 Supernatants were also analyzed by AF<sup>4</sup>-UV-ICPMS following the operational conditions  
26 detailed in Table 1.  
27  
28  
29  
30  
31  
32  
33  
34  
35  
36  
37  
38  
39  
40  
41

### 42 **3. Results and discussion.**

#### 43 **3.1 Synthesis of chitosan-modified selenium nanoparticles.**

44  
45 Radish plants were hydroponically grown in presence of Chitosan-modified SeNPs.  
46 Nanoparticles were synthesized in the laboratory through the reduction of selenite with  
47 ascorbic acid using chitosan as stabilizer. The method is based on those reported by Bay *et al*  
48 <sup>9</sup> and Zang *et al*<sup>10</sup> where water-soluble polysaccharides (chitosan, konjac glucomannan,  
49 carboxymethyl cellulose, and acacia gum) were used as modifiers or stabilizers of SeNPs.  
50 The resulting SeNPs suspensions were stable up to 6 months of storage. We evaluated the  
51 following experimental parameters: chitosan concentration, ascorbic concentration and initial  
52  
53  
54  
55  
56  
57  
58  
59  
60



1  
2  
3 pH value of chitosan solution. Optimization was performed by applying a univariate  
4 approach. Several Chitosan (0.01 – 0.5% (w/v)) and ascorbic acid (0.027M, 0.054M,  
5 0.108M, 0.27M and 0.34M) concentrations were tested for preparing CS-SeNPs. The best  
6 conditions for obtaining spherical CS-SeNPs with an efficiency of formation (calculated as  
7 indicated in section 2.2) higher than 95% were: 0.1% chitosan, 0.034M ascorbic acid, 0.24M  
8 acetic acid and pH=5.

9  
10  
11 pH-value results to be one of the most relevant parameters when using chitosan. Chitosan  
12 with a pKa of 6.3 is polycationic when dissolved in acid and presents  $\text{NH}_3^+$  sites. It is  
13 expected that the pH of the chitosan solution would play a significant role. Results shown in  
14 Fig.1A revealed that the smallest CS-SeNPs were obtained when the synthesis pH decreases  
15 from 6 to 3. At  $\text{pH} \geq \text{pKa}$ , SeNPs begun to aggregate as it is shown in TEM images in Fig.1B.

16  
17  
18  
19  
20  
21  
22  
23 Diameter and shape of the synthesized NPs was measured by using TEM. The term particle  
24 sizes in this paper refer to the average diameter of the CS-SeNPs. The average diameter of  
25 the spherical CS-SeNPs was determined based on the diameter of about a hundred particles  
26 from the TEM micrographs for each sample. SeNPs with an average diameter of  $25 \pm 5 \text{nm}$   
27 were obtained under these conditions according to transmission electron microscopy results  
28  
29  
30  
31

### 32 33 **3.3. CS-SeNPs accumulation and biotransformation in Se-enriched radish.**

34  
35  
36 Accumulation and biotransformation of selenium by plants have been reported in several  
37 papers.<sup>1,8,11</sup> Many *Allium* (*Allium cepa* L., *Allium sativum* L., *Allium schoenoprasum* L., etc.)  
38 and *Cruciferae* species (*Brassica juncea* and *Brassica oleracea*) have been the subject of  
39 several studies as they are able to incorporate high quantities of selenium and to produce  
40 seleno amino acids, which are potentially bioactive for nutrition purposes and  
41 phytoremediation. Most of published scientific research papers involved selenite and/or  
42 seleniate as sources of selenium. In general a low transformation of selenium into organic  
43 forms is observed in plants grown in Se(VI)-enriched culture media. On the contrary, in those  
44 plants exposed to selenite, most of selenium added is transformed into seleno amino acids.  
45 Some of the organic compounds identified in different plants tissues are: selenomethionine,  
46 selenocystine,  $\gamma$ -glutamyl selenomethylselenocystine, selenomethyl selenocysteine,  
47 selenocystathione, selenohomocysteine and selenomethylselenomethionine. Both  
48 selenocysteine and selenomethionine can be incorporated into the proteins, which can leads  
49  
50  
51  
52  
53  
54  
55  
56  
57  
58  
59  
60

1  
2  
3 to phytotoxicity. However, selenomethylselenocysteine is a non-proteinogenic seleno amino  
4 acid, which has been identified in plants that exhibit a quite tolerance to selenium.

5  
6 As abovementioned, all studies have been conducted in plants hydroponically grown in  
7 Se(IV) and Se(VI)-enriched media but few data about SeNPs accumulation and  
8 transformation in plant systems is available in the literature. With the aim of gaining a deeper  
9 insight into how SeNPs are accumulated and biotransformed in plants, radish plants were  
10 hydroponically grown in presence of CS-SeNPs and selenite, for comparison purposes.  
11 Radishes (*Raphanus sativus*) were selected as being one of the commonest of garden  
12 vegetables because of the ease and rapidity with which crop may be obtained. Afterwards, the  
13 resulting plants were analyzed by ICPMS for the quantitative determination of total selenium,  
14 by HPLC-ICPMS for the identification and determination of selenium species and by AF<sup>4</sup>-  
15 UV-ICPMS for the size characterization of CS-SeNPs in the root system. The ICPMS and  
16 HPLC-ICPMS methods were validated by using an enriched wheat flour reference material  
17 (ERM BC210a), certified for selenium ( $17.23 \pm 0.91 \mu\text{g g}^{-1}$ ) and SeMet ( $27.4 \pm 2.6 \mu\text{g g}^{-1}$ ).  
18 Because, at 95 % confidence, no significant differences were observed between the certified  
19 value and the experimental ones, the method was believed accurate for total selenium  
20 determination and selenium speciation, respectively.  
21  
22  
23  
24  
25  
26  
27  
28  
29  
30  
31  
32

33 Total selenium concentration found in radish hydroponically grown in selenium-enriched  
34 media was:  $207 \pm 2$  and  $144 \pm 4 \mu\text{g Se g}^{-1}$  when supplementing Se as selenite or as selenium  
35 nanoparticles, respectively. Selenium accumulation was a 25% higher in those plants grown  
36 in selenite. No perceptible symptoms of toxicity were detected in plants grown in both  
37 selenite and CS-SeNPs media. Once selenium accumulation was evaluated, selenium species  
38 were extracted by means of an enzymatic treatment using ultrasound probe sonication (USP)  
39 following the procedure detailed in the experimental section. The resulting extracts were  
40 further analyzed by using two separation mechanisms: anion exchange and reversed phase  
41 chromatography on line coupled to ICPMS. In terms of recovery for the column, all of the  
42 selenium was quantitatively recovered ( $100 \pm 4$ ) from the injection of selenium species  
43 standards. The chromatograms of selenium species obtained by anion-exchange and reversed  
44 phase chromatography corresponding to radish grown in presence of selenite and CS-SeNPs  
45 are shown in Fig. 2. The main species found in the chromatograms, by comparison of the  
46 retention time of the standards and by spiking experiments were MeSeCys and SeMet. The  
47 chromatograms profiles obtained from radish extracts were independent on the chemical form  
48 in which selenium was supplemented to radish plants. Quantification of Selenium species  
49  
50  
51  
52  
53  
54  
55  
56  
57  
58  
59  
60

1  
2  
3 was performed by using HPLC-ICPMS. Table 2 shows the concentration of Se-species and  
4 the fraction of total selenium (calculated as the sum of selenium in separated Se species  
5 relative to the total Se extracted. Recovery values ranged from 95 to 100%, suggesting CS-  
6 SeNPs transformation to organic selenium compounds once CS-SeNPs has been taken by  
7 radish plants and by following a similar metabolic pathway to selenite. The most likely  
8 reason for the high CS-SeNPs tolerance observed in these plants is the formation of MeSeCys  
9 a non proteinogenic seleno amino acid linked with selenium detoxification processes in  
10 plants.  
11  
12  
13  
14  
15  
16  
17

### 18 **3.4. Characterization of CS-SeNPs in radish root system by AF<sup>4</sup>-UV-ICPMS and TEM.**

19  
20  
21 As CS-SeNPs was not detected inside radish, it can be hypothesized that the CS-SeNPs could  
22 be transformed on/ in the root surface. Radishes present a tap root system structure which is  
23 made up of a central large root that is called the taproot (the edible part) and lateral roots  
24 (smaller in diameter than the taproot), which originate from the pericycle, branch off from the  
25 taproot, and subsequent lateral roots can branch off other lateral roots. With the aim of  
26 gaining a deeper insight in CS-SeNPs metabolic pathway, the presence of CS-SeNPs on the  
27 surface of the taproot (the edible part) and lateral roots of the radish plants was evaluated by  
28 TEM measurements after extracting SeNPs from radish roots by using the medium previously  
29 employed for the synthesis of CS-SeNPs (0.1% Chitosan, 0.034M Ascorbic acid, 0.24M  
30 Acetic acid) as extracting solution. TEM images of CS-SeNPs extracted from lateral roots  
31 (Fig.3A) show the presence of spherical selenium nanoparticles with a particle diameter  
32 estimated of 25±8nm. However, TEM images of CS-SeNPs extracted from taproot (Fig. 3B)  
33 shows that particles are mainly interconnected, assembled or aggregated. XEDS analysis of  
34 the selected regions confirms the presence of selenium in particles composition. The results  
35 suggest that CS-SeNPs begins to aggregate on the tap root surface and then transformed into  
36 selenium organic species in taproot.  
37  
38  
39  
40  
41  
42  
43  
44  
45  
46  
47

48 Once size and morphology of CS-SeNPs was studied by TEM, the capability of AF<sup>4</sup> on line  
49 coupled to UV and ICPMS for determining CS-SeNPs size in the root system of the radish  
50 was evaluated. The optimized AF<sup>4</sup> settings and flows used for nanoparticles fractionation and  
51 the UV and ICPMS detection operating conditions are detailed in Table 1. Under these  
52 separation conditions, the recovery of the fractionation method was calculated following an  
53 on-line approach where sample is injected both with and without applying a cross-flow field.  
54  
55  
56  
57  
58  
59  
60

1  
2  
3 Afterwards, the area under each peak is integrated, and the difference represents the analyte  
4 mass loss in the channel. In our case, the recovery was set at  $R (\%) \approx 95 \pm 5$ .

5  
6 To date obtaining adequate information on NPs sizes is still an important issue in  $AF^4$   
7 analysis. It is known that the separation of NPs in  $AF^4$  channel occurs according to their  
8 diffusion coefficient which can in turn be related to the hydrodynamic particle size or  
9 molecular weight. Different strategies have been proposed to determine the hydrodynamic  
10 diameter of fractionated particles, such as by applying FFF theory or by using certified  
11 standards in size to “calibrate” the retention time-size dependence for a specific set of flow  
12 conditions. Both approaches entail that size fractionation is only dependent on the size of the  
13 component but independent of its chemistry. However, erroneous information may still be  
14 obtained since these calibration methods do not take into account elution time changes due to  
15 specific NP-membrane interactions, different behavior between the NPs used for calibration  
16 and the analyte, formation of aggregates and nature of the nanoparticles<sup>12,13</sup>. Recently,  
17 Gigaut *et al*<sup>14</sup> have shown the influence of the core NP material nature on the retention  
18 process in the  $AF^4$  channel. For the same size, it appears that the retention time increases with  
19 the bulk or core density of NPs (Au Ag). However, this effect was not observed for nominally  
20 size-matched low density materials such as PLS and SeNPs which appeared in the fractogram  
21 at a similar retention time. Based on that, we developed a size calibration procedure using  
22 polystyrene latex beads reference standards of three known sizes (22, 54 and 100 nm)  
23 (Fig.4A). The equation obtained for the calibration was: diameter (nm)= 2,073  $t_r$ (min) +  
24 9,893 and the correlation coefficient ( $r^2$ ) was 0.9932 which was considered suitable for  $AF^4$   
25 calibration. Before applying the equation to estimate CS-SeNPs diameter size in the radish  
26 root system, the method was tested to determine the size of the synthesized CS-SeNPs. The  
27 size was estimated to be  $26 \pm 3$ nm (Fig. 4B) which indicates good agreement with the values  
28 provided by TEM ( $25 \pm 5$ nm) measurements.

29  
30 The root extracts containing CS-SeNPs were injected into the  $AF^4$ -UV-ICPMS system and  
31 analyzed by using the previously optimized separation conditions. Fractograms obtained are  
32 shown in Fig. 5. In case of lateral roots (Fig. 5A), the fractogram shows 2 peaks at retention  
33 time of 7.1 and 8.7min corresponding to an estimated diameter (based on polystyrene latex  
34 beads reference standards retention time) of  $29 \pm 4$  and  $33 \pm 6$  nm, respectively. These results  
35 are in agreement with those provided by using TEM ( $25 \pm 8$ nm). On the other hand, in taproot  
36 extract where selenium is present as isolated and aggregated CS-SeNP, two peaks were  
37 obtained in the fractogram (Fig. 5B). The first peak appeared at 5-6,5 minutes and may  
38 correspond to isolated CS-SeNPs with an estimated diameter (based on polystyrene latex  
39  
40  
41  
42  
43  
44  
45  
46  
47  
48  
49  
50  
51  
52  
53  
54  
55  
56  
57  
58  
59  
60

1  
2  
3 beads reference standards retention time) of  $26\pm 3$  nm which is in agreement with the results  
4 obtained by TEM. The second peak appeared at 17-28 min, it was quite broad and could  
5 correspond to aggregated CS-SeNPs with an estimated hydrodynamic diameter of 55 nm.  
6 However, sometimes, elution times provided by AF<sup>4</sup> cannot be associated with the real size  
7 of the NPs, e.g., especially when NPs are aggregated.  
8  
9

10  
11  
12 Very few references exist on NPs transformations in plants. Biotransformation is a critical  
13 factor that may modify the toxicity, behavior, and fate of engineered nanoparticles in the  
14 environment. In the case of ZnO NPs, results revealed that Zn was found inside the soybean  
15 plant only as Zn<sup>2+</sup><sup>15</sup>. Stampoulis *et al.*<sup>16</sup> reported that Ag was found at a greater concentration  
16 in zucchini grown in Ag NPs than those cultivated in Ag bulk solution, no test was done to  
17 determine whether the Ag, existed as NPs. Yin *et al.*<sup>17</sup> found that the silver speciation in the  
18 roots of Ag NPs exposed *Lolium multiflorum* was oxidized to Ag(I). Zhan *et al.*<sup>18</sup> report  
19 transformation of the high stable CeO<sub>2</sub> NPs in the cucumber plants. The authors speculate  
20 that CeO<sub>2</sub> NPs were first absorbed on the root surfaces and partially dissolved with the  
21 assistance of the organic acids (citric acid) and reducing substances (ascorbic acid) excreted  
22 by the roots. From the results obtained in the present work we can assume that CS-SeNPs are  
23 once dissolved and transformed into inorganic selenium, and then, metabolized to organic  
24 selenium compounds following a similar metabolic pathway to selenite.  
25  
26  
27  
28  
29  
30  
31  
32  
33  
34  
35  
36  
37

#### 38 **4. Conclusions**

39 Results shown that the stable CS-SeNPs are biotransformed in exposed radish being a  
40 percentage higher 95% of CS-SeNPs applied biotransformed into MetSeCyst and SeMet.  
41 Similar results were obtained when selenium was supplemented as selenite which allow us to  
42 think that transformation occurs in the same manner. TEM images from the root radish  
43 system revealed the presence of CS-SeNPs on root systems, suggesting selenium  
44 transformation takes place inside radish. The size distributions of CS-SeNPs in root radish  
45 system, determined by TEM, were in good agreement with that obtained from AF<sup>4</sup>-ICPMS.  
46 These results are of importance since the number of applications of AF<sup>4</sup>-ICPMS to size  
47 characterization of NPs in living systems is scarce. Results presented in this manuscript  
48 highlight the importance of the biological system in the transformation of nanoparticles. The  
49 modification of nanoparticles in the transformation will not only change their fate and  
50  
51  
52  
53  
54  
55  
56  
57  
58  
59  
60

1  
2  
3 toxicity, but also may cause dysfunction of their beneficial application such as delivery  
4 system.  
5  
6

## 7 8 **Acknowledgments**

9  
10 The authors thank the Spanish Commission of Science and Technology (CTQ2011-22732),  
11 the Community of Madrid/ FEDER programme (S2013/ABI-3028, AVANSECAL-CM) and  
12 the UE/ FEDER Interreg Project Orque Sudoe. (Ref: SOE3/P2/F591) for funding.  
13  
14  
15  
16  
17

## 18 19 **References**

- 20  
21 1. Z. Pedrero and Y. Madrid, *Anal. Chim. Acta*, 2009, **634**, 135-152  
22  
23 2. MI Lopez-Heras, M. Palomo and Y. Madrid, *Anal. Bional. Chem.*, 2011, **400**, 1717-1727.  
24  
25 3 M.I. Jackson and G.F. Jr Combs, *Curr Opin Clin Nutr Metab Care* , 2008, **11**, 718-726.  
26  
27 4. J. Zhang, X. Wang and T. Xu, *Toxicol. Scie.*, 2008,**101**, 22-31.  
28  
29 5 I. Lopez-Heras, R. Sanchez-Diaz, D. S. Anunciação, Y. Madrid, J. L. Luque-Garcia and C.  
30 Camara. *J. Nanomed. Nanotechnol.*, 2014, **5**, 226.  
31  
32 6 A. Romero-Pérez , E. García-García , A. Zavaleta-Mancera J. E. Ramírez-Bribiesca , A.  
33 Revilla-Vázquez, L. M. Hernández-Calva , R. aquel López-Arellano and R. G. Cruz-  
34 Monterrosa. *Vet Res Commun* , 2010, **34**,71–79.  
35  
36 7 E. Domokos-Szabolcsy, L. Marton, A. Sztrik , B. Babka, J. Prokisch, and M. Fari. *Plant*  
37 *Growth Regul.*, 2012, **68**, 525–531.  
38  
39 8 Z. Pedrero, Y. Madrid and C. Cámara, *J. Agric. Food Chem.*, 2006, **54**, 2412-17.  
40  
41 9 Y. Bai, Y. Wang, W. Zhou, Li and W. Zheng, *Material Letters*, 2008, **62**, 2311-2314.  
42  
43 10 Z. Sheng-Yi, Z. Juan, W. Hong-Yan and C. Hong-Yuan. *Materials Letters*, 2004, **58**,  
44 2590– 2594  
45  
46 11. MM. Seppänen, J. Kontturi, I. Lopez- Heras, Y. Madrid, C. Camara and H. Hartikainen.  
47 *Plant. Soil*, 2010, **337**, 273-283.  
48  
49  
50  
51  
52  
53  
54  
55  
56  
57  
58  
59  
60

- 1  
2  
3 12 A. Ulrich, S. Losert, N. Bendixen, A. Al –Kattan, H. Hagendorfer, B. Nowack, C. Adlhart,  
4  
5 J. Ebert, M. Lattuadae and K.J.Hungerbuhler. *J. Anal. Atom. Spectrom.* 2012, **27**,1120-1130.  
6  
7 13 I. López-Heras, Y. Madrid and C. Cámara, *Talanta*, 2014, **124**,71-78.  
8  
9 14 J. Gigault and V. A. Hackley. *Anal and Bional. Chem.*, 2013, **405**, 6251–6258.  
10  
11 15 M.L. López-Moreno, G. De La Rosa, J.A. Hernandez-Viezcas, H. Castillo-Michel, C.E.  
12 Botez, J.R. Peralta- Videa and J.L .Gardea-Torresdey, *Environ Sci Technol.*, 2010, **44**, 7315–  
13 7320.  
14  
15 16 D. Stampoulis, S.K. Sinha and J.C. White. *Environ. Sci. Technol.*, 2009, **43**, 9473–9479.  
16  
17 17 L.Yin, Y. Cheng, B. Espinasse, B. P. Colman, M. Auffan, M.Wiesner, J. Rose, J. Liu and  
18 E. S. Bernhardt. *Environ. Sci. Technol.*, 2011, **45**, 2360–2367.  
19  
20 18 P. Zhang, Y. Ma, Z. Zhang, X. He, J. Zhang, Z. Guo, R. Tai, Y. Zhao, and Z. Cha.  
21 *ACS Nano*, 2012, **6**, 9943-9950.  
22  
23  
24  
25  
26  
27  
28  
29  
30  
31  
32  
33  
34  
35  
36  
37  
38  
39  
40  
41  
42  
43  
44  
45  
46  
47  
48  
49  
50  
51  
52  
53  
54  
55  
56  
57  
58  
59  
60



**Table 1** Operating Conditions for HPLC and A4F coupled to ICPMS

<b>Operating Conditions</b>	
<b>ICPMS parameters</b>	
RF Power (W)	1550
Plasma gas flow rate (L min <sup>-1</sup> )	15.0
Ar auxiliar flow rate (L min <sup>-1</sup> )	0.30
Carrier gas flow rate (L min <sup>-1</sup> )	0.75
Nebulizer	Conikal
Spray Chamber	Scott
Adquisition mode	Continuos
Isotopes monitored	<sup>76</sup> Se, <sup>77</sup> Se, <sup>78</sup> Se, <sup>80</sup> Se
Replicates	3
Reaction gas	H <sub>2</sub>
Reaction gas (mL H <sub>2</sub> min <sup>-1</sup> )	6
<b>AEX chromatographic parameters</b>	
Column	Hamilton PRP X-100 (150mmx4.6mm, 10μm)
Mobile phases	Ammonium citrate 10mM, 2%MeOH (pH 5.0)
Mode	Isocratic
Flow rate (mL min <sup>-1</sup> )	1
Injection volume (μL)	100
<b>RP chromatographic parameters</b>	
Column	Zorbax C8 (250 x 4.60 mm, 5μm)
Mobile phases	2% MeOH, 0.1% TFA (pH 2.2)
Mode	Isocratic
Flow rate (mL min <sup>-1</sup> )	1
Injection volume (μL)	100
<b>AF4 separation parameters</b>	

Membrane	Cellulose regenerated (10kDa Cut-off filter)
Spacer (nm)	500
Mobile phases	Water
Injection flow (mL min <sup>-1</sup> )	0.1
Injection time (min)	2
Cross flow (mL min <sup>-1</sup> )	2
Gradient mode	Power (Exponential 0.5)
Injection volume (μL)	200
Wavelength (nm)	369

1  
2  
3  
4  
5  
6  
7  
8  
9  
10  
11  
12  
13  
14  
15  
16  
17  
18  
19  
20  
21  
22  
23  
24  
25  
26  
27  
28  
29  
30  
31  
32  
33  
34  
35  
36  
37  
38  
39  
40  
41  
42  
43  
44  
45  
46  
47  
48  
49  
50  
51  
52  
53  
54  
55  
56  
57  
58  
59  
60

**Table 2** Concentration ( $\mu\text{g Se g}^{-1}$ ) of selenium-species contained in control and Se-enriched radish.

Sample	MeSeCys $x \pm s^a$ ( $\mu\text{g Se g}^{-1}$ )	MeSeCys R (%) <sup>b</sup>	SeMet, $x \pm s^a$ ( $\mu\text{g Se g}^{-1}$ )	SeMet, R (%) <sup>b</sup>	SeOMet, $x \pm s^a$ ( $\mu\text{g Se g}^{-1}$ )	SeOMet, R (%) <sup>b</sup>	Fraction of Total selenium
<b>Anion exchange chromatography-ICPMS</b>							
Control	0.221 $\pm$ 0.001	21.6 $\pm$ 0.5	0.557 $\pm$ 0.008	54.4 $\pm$ 0.9	0.25 $\pm$ 0.02	24 $\pm$ 1	
Se(IV) treated- radish	72.29 $\pm$ 0.02	64.2 $\pm$ 0.2	32.2 $\pm$ 0.4	28.6 $\pm$ 0.5	8.1 $\pm$ 0.8	7.2 $\pm$ 0.7	103 $\pm$ 4
CS-SeNPs treated- radish	43 $\pm$ 1	55.3 $\pm$ 0.1	27 $\pm$ 1	35.2 $\pm$ 0.5	7.3 $\pm$ 0.5	9.5 $\pm$ 0.6	91 $\pm$ 4
<b>Reversed phase chromatography_ICPMS</b>							
Control	0.70 $\pm$ 0.02	66 $\pm$ 1	0.264 $\pm$ 0.002	26.3 $\pm$ 0.2	0.1 $\pm$ 0.01	7.8 $\pm$ 0.3	
Se(IV) treated- radish	47 $\pm$ 1	70 $\pm$ 1	16.5 $\pm$ 0.3	24.9 $\pm$ 0.4	2.94 $\pm$ 0.06	4.4 $\pm$ 0.2	99 $\pm$ 3
CS-SeNPs treated- radish	35.1 $\pm$ 0.5	67.3 $\pm$ 1	14.2 $\pm$ 0.3	27.2 $\pm$ 0.6	2.9 $\pm$ 0.3	5.5 $\pm$ 0.5	97 $\pm$ 4

<sup>a</sup> Average value  $\pm$  standard deviation (n=3)<sup>b</sup> Distribution of Se species. R(%) denotes the ratio of Se species concentration to total selenium extracted<sup>c</sup> The fraction of total Se (%) denotes the ratio of the sum of Se species concentrations to total selenium extracted.In terms of recovery for the column, all of the selenium was quantitatively recovered (100 $\pm$ 4) from the injection of selenium species standard

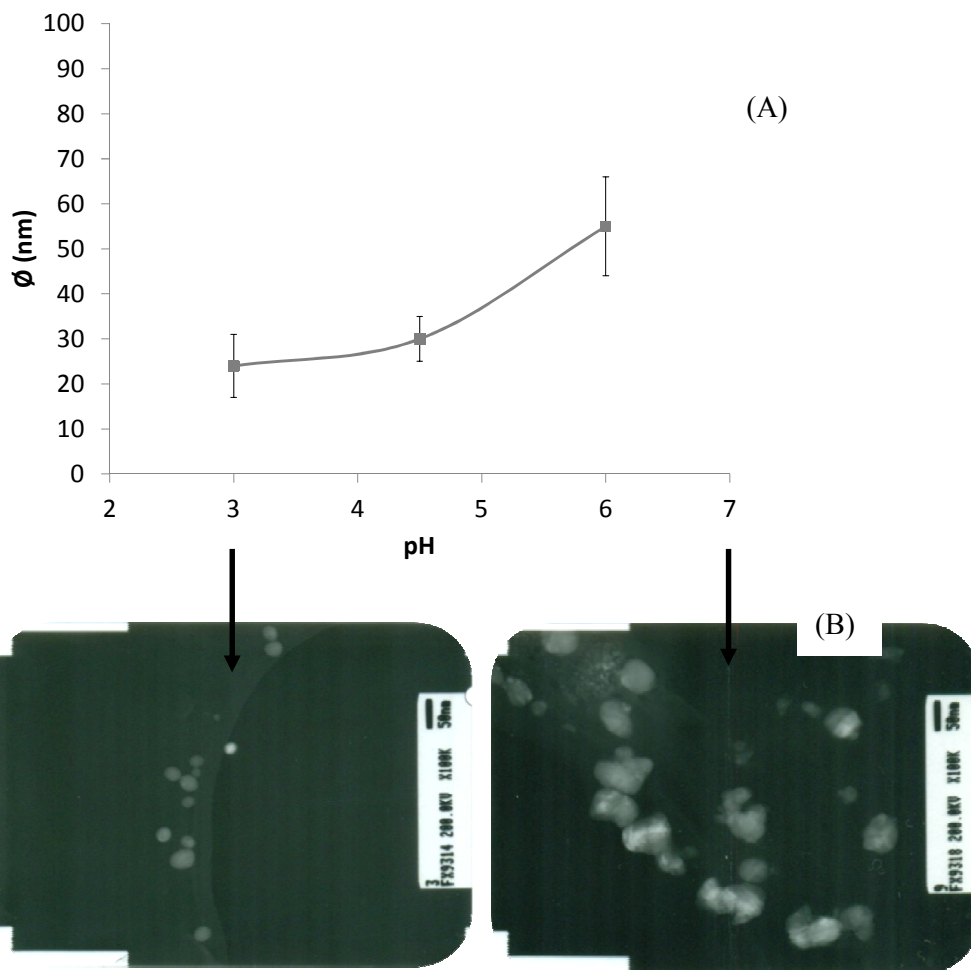
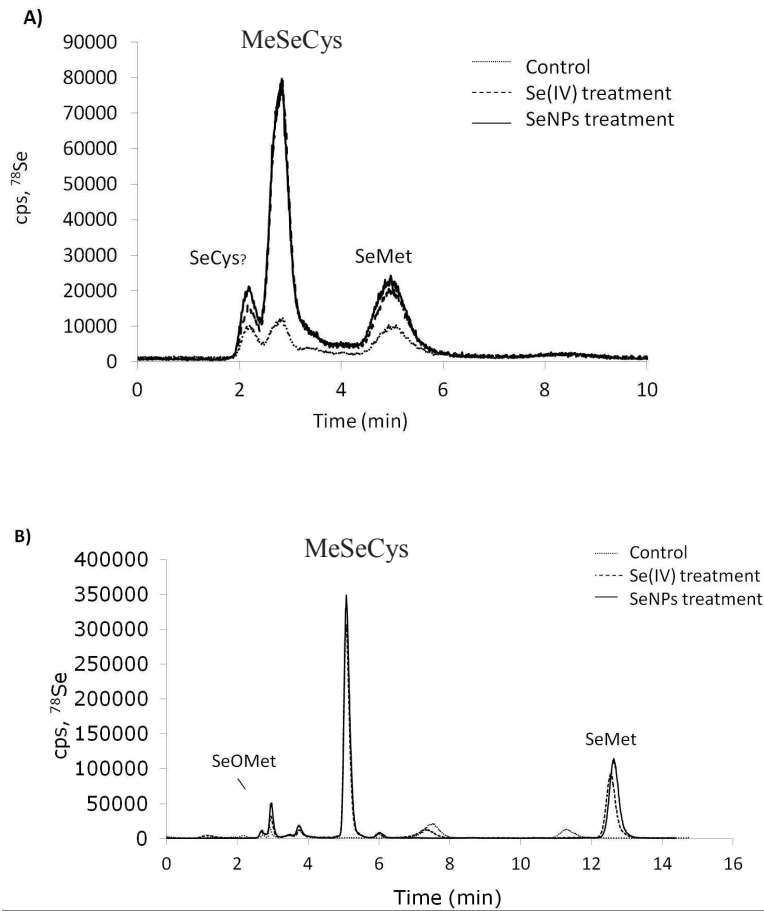


Figure 1

**Figure 2**

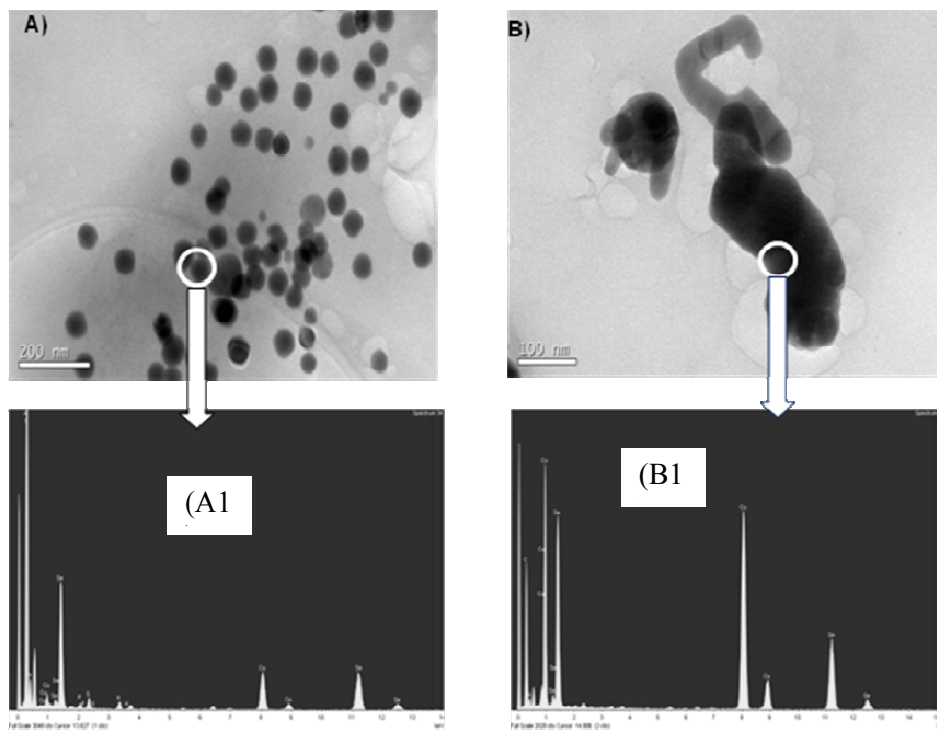
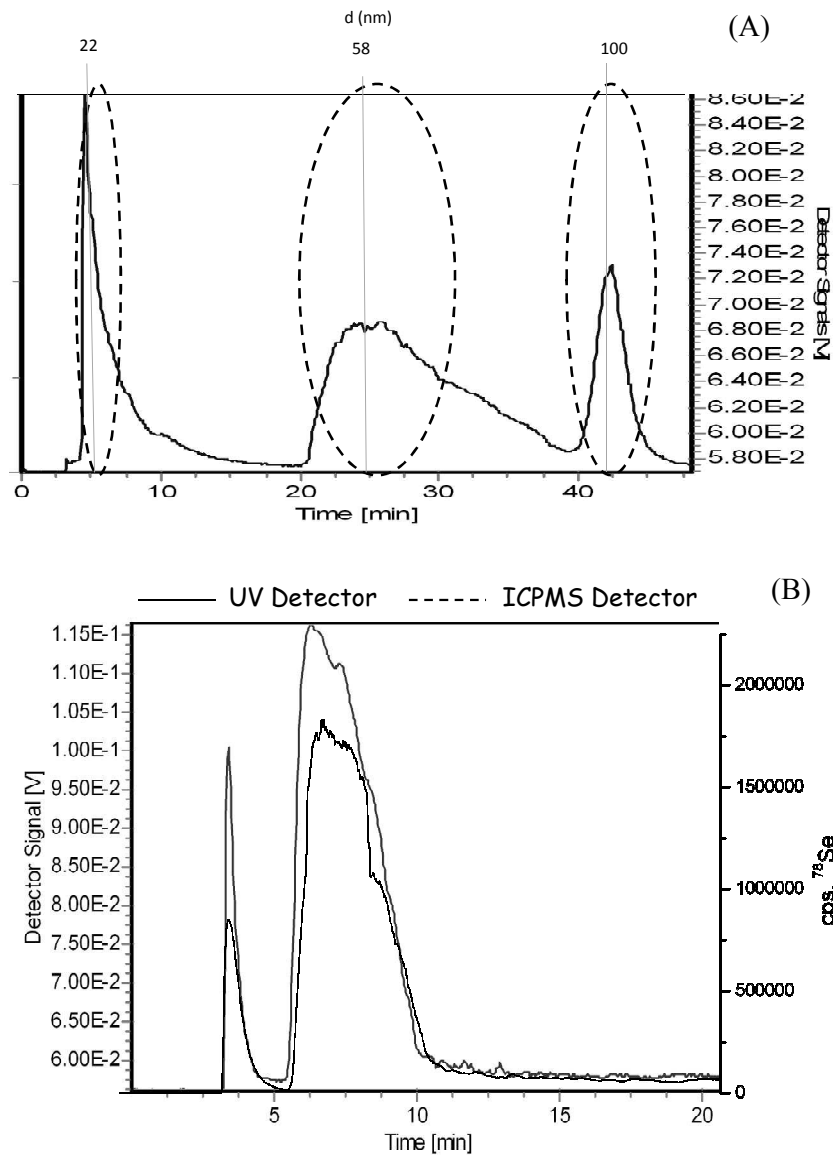
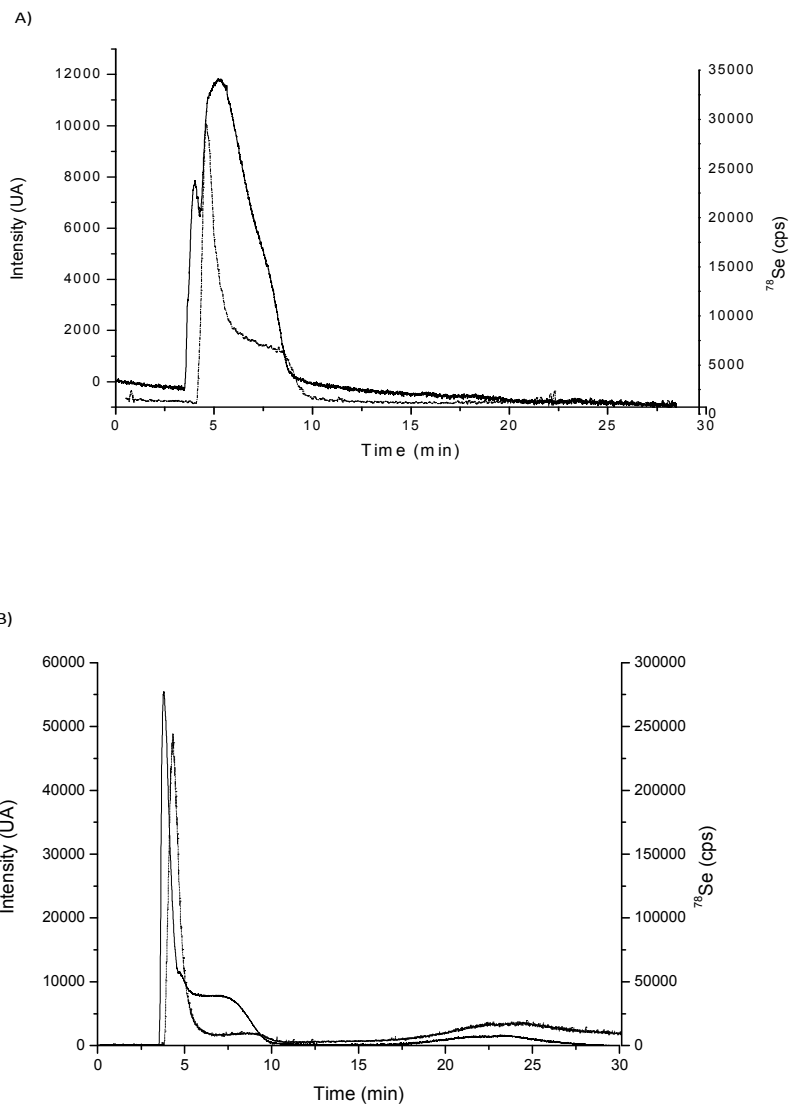
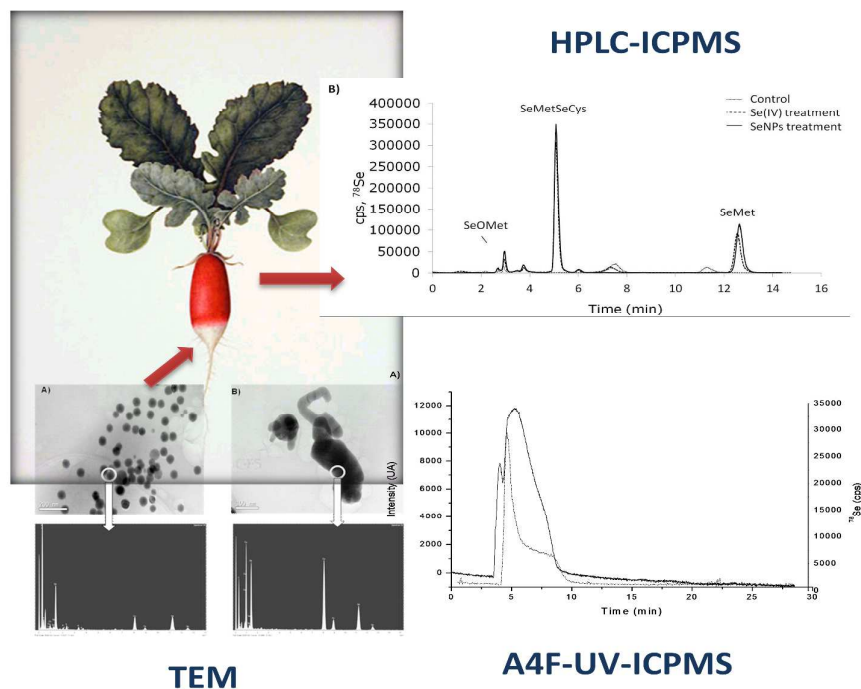


Figure 3





**Figure 5**



Biotransformation of chitosan- modified SeNPs (CS-SeNPs) in radish plants (*Raphanus sativus*) was performed by using an analytical methodology which combines high performance liquid chromatography (HPLC) and asymmetrical field flow fractionation (A4F) on line coupled to inductively coupled plasma mass spectrometry (ICP-MS) as well as transmission electron microscopy (TEM).